ROYAL SOCIETY OF CHEMISTRY

PAPER

Check for updates

Unraveling the role of the electron-pair density symmetry in reaction mechanism patterns: the Newman–Kwart rearrangement†

Leandro Ayarde-Henríquez, [ID] * Cristian Guerra, Mario Duque-Noreña and Eduardo Chamorro [ID] *

This work focuses on correctly identifying the topological signatures associated with the bond-breaking/bond-forming processes along the versatile Newman–Kwart rearrangement. In contrast to recent reports and within the framework of the so-called bonding evolution theory, we show that only fold bifurcations emerge based on a detailed examination of the Hessian value at all potentially degenerate critical points and their relative distances along the pathway. The chemical implications of incorrectly classifying the nature of chemical events are outlined.
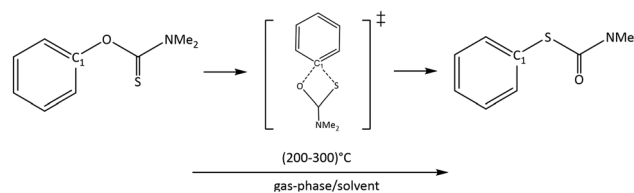
Introduction

The works of Kwart and Evans,[1] on the one hand, and Newman and Karnes,[2] on the other, led to the identification of the molecular mechanism we now call the Newman–Kwart rearrangement (NKR). The NKR is a thermally induced process encompassing the migration of *O*-aryl thiocarbamates to the corresponding *S*-aryl compounds,[3–9] as depicted in Scheme 1.

High temperatures are required to overcome the energy activation barrier ranging from 35 to 43 kcal mol^{-1};[5,9,10] however, such temperature values lead to some difficulties that decrease the reaction's organic synthesis potential.[5,9,10] Despite these drawbacks, the NKR has been extensively investigated from both experimental and theoretical approaches, providing a broad range of applications in critical areas, including supramolecular chemistry,[11,12] pharmaceutical intermediates,[13,14] dyes,[15] molecular switches,[16] and chiral ligand synthesis,[17,18] among others.

From a theoretical/computational point of view, several modern interests based on the applications of density functional theory (DFT)[19] are simply oriented to probe whether the aromatic migration $O_{Ar} \rightarrow S_{Ar}$ (see Scheme 1) proceeds *via* a four-membered transition state,[3] or to elucidate the activation barriers.[6,9] Curiously, much less attention has been devoted to studying the remarkable features of the electron density flow driving the transformation. A deeper understanding of the NKR

mechanism requires detailed knowledge concerning electron reorganization to reveal the underlying essential bonding sequences. It should be emphasized that topological methods have provided a solid framework for investigating a wide variety of bonding situations, providing new and unexpected chemical insights.[20] Within this context, Zahedi *et al.*[21] recently described the forming/breaking processes of a chemical bond featuring the NKR using DFT machinery and bonding evolution theory (BET).[22] BET is aimed at characterizing electron-pair rearrangements along a reaction pathway in terms of a set of parametric polynomials (called unfoldings) derived from Thom's catastrophe theory.[23] Using this topological approach, Zahedi *et al.*[21] rationalized the NKR molecular mechanism displayed in Scheme 1 *via* three unfoldings: a fold, an elliptic umbilic, and a cusp. The first polynomial characterizes the onset of the electron pairing reorganization leading to a simple bond between the ipso–carbon C1 and the sulphur atom. The second one describes the C1–O breaking process, whereas the C1–S final formation occurs through a cusp function.

Following recent advancements in the field, we reproduced all calculations by carefully following their setup. Contrary to

Universidad Andrés Bello, Facultad de Ciencias Exactas, Departamento de Ciencias Químicas, Avenida República 275, 8370146, Santiago de Chile, Chile.
E-mail: l.ayardehenriquez@uandresbello.edu, echamorro@unab.cl

† Electronic supplementary information (ESI) available: Complete theoretical and methodological details, optimized parameters, plots of the Hessian matrix value, *etc.* See DOI: https://doi.org/10.1039/d2nj01501c

Scheme 1 The Newman–Kwart mechanism is traditionally rationalized in terms of an intramolecular electronic rearrangement *via* a four-membered cyclic transition state.

previous findings, we found that only fold-type polynomials can be correctly identified, consistent with our previous observations, both in the ground[20] and electronically excited states.[24–26] This work focuses on the rigorous assignment of unfoldings characterizing relevant chemical events along the intrinsic reaction coordinate (IRC) featuring the NKR. For details regarding the electron population of ELF basins and the aromatic behaviour of the benzene ring along the reaction pathway, the reader should refer to the results already discussed in the work of Zahedi *et al.*[21] On the other hand, our BET-type analysis shows that the C1–S bond forms before the C1–O breaks, contrary to the report of Zahedi *et al.* We also aim to point out the chemical implications of our results.

Results and discussion

Fig. 1 depicts two extended molecular graphs for the electron localization function (ELF).[27] Near the critical point (CP) of index one, s_{1_1}, appears a pair of new CPs, namely, the attractor a_6 and the saddle s_{1_2}. The relative distance between this maximum and s_{1_1}, a_6–s_{1_1}, is 1.6 times greater than a_6–s_{1_2},

and consequently, the Hessian matrix at s_{1_1} is about 3 times greater than the value at the attractor. These results indicate that s_{1_1} is not linked with such a change in the number of ELF CPs. Therefore, a fold polynomial constitutes a suitable tool for describing this electron-pair reorganization, as argued by Zahedi *et al.*[21]

As the reaction progresses, the subsequent two folds take place non-simultaneously. Firstly, the valence shell of the sulphur atom splits, and the (a_7, s_{1_3}) pair appears. Since no other CP is close enough, such a chemical event must be characterized *via* a fold function, as shown in Fig. 2(a and b). Then, the loss of one of the lone pairs of the oxygen occurs *via* the third fold due to a_4 colliding with s_{1_4}, and both points disappear (Fig. 2(b and c)).

Because of the continuous approach of the attractor a_6 and the saddle of index one s_{1_5}, these critical points coalesce through a fold-type polynomial, as shown in Fig. 3. In other words, the simplest unfolding of Thom's theory[23] reasonably characterizes the formation of a simple bond between the C1 ipso–carbon and the sulphur atom. No flag of a cusp unfolding is detected since this topographical event encompasses only two critical points; consequently, the number of ELF CPs
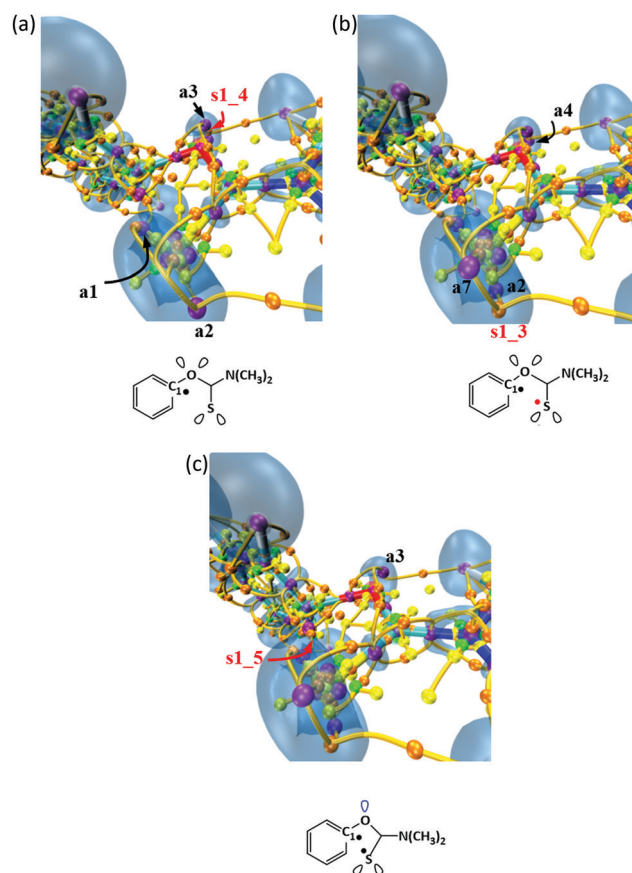

Fig. 1 Extended ELF-molecular graphs together with the Lewis-like structures, including all types of ELF CPs: attractors or maxima in purple, saddles of index one in orange, saddles of index two in yellow and minima or repellors in green; (a) before and (b) after the first change. The ELF isosurface (0.85) is also shown.

Fig. 2 Extended ELF-molecular graphs together with the Lewis-like structures, including all types of ELF CPs: attractors or maxima in purple, saddles of index one in orange, saddles of index two in yellow and minima or repellors in green; (a and b) before and (b and c) after the second and third changes. The ELF isosurface (0.85) is also shown.
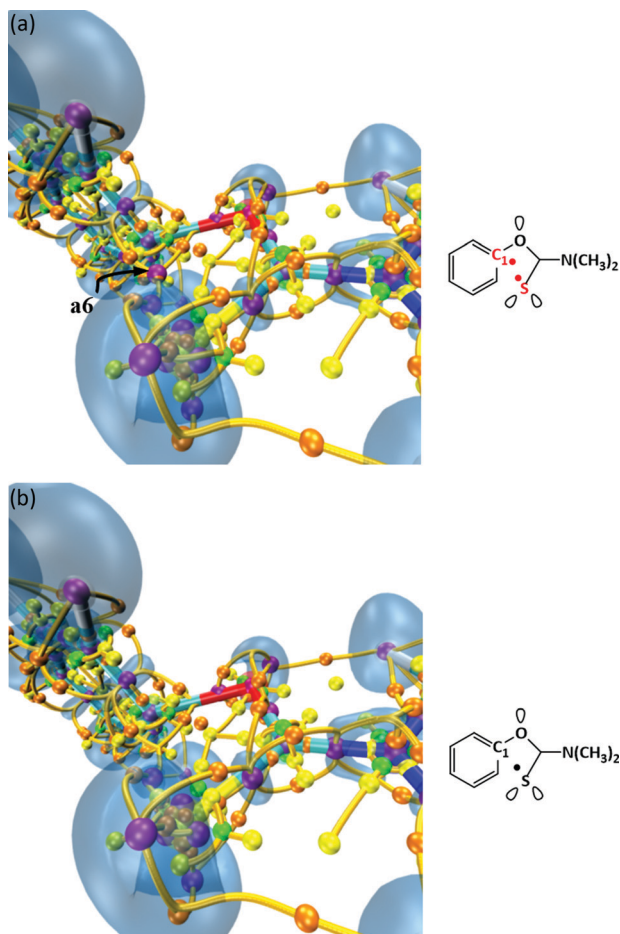
Fig. 3 Extended ELF-molecular graphs together with the Lewis-like structures, including all types of ELF CPs: attractors or maxima in purple, saddles of index one in orange, saddles of index two in yellow and minima or repellors in green; (a) before and (b) after the fourth change. The ELF isosurface (0.85) is also shown.
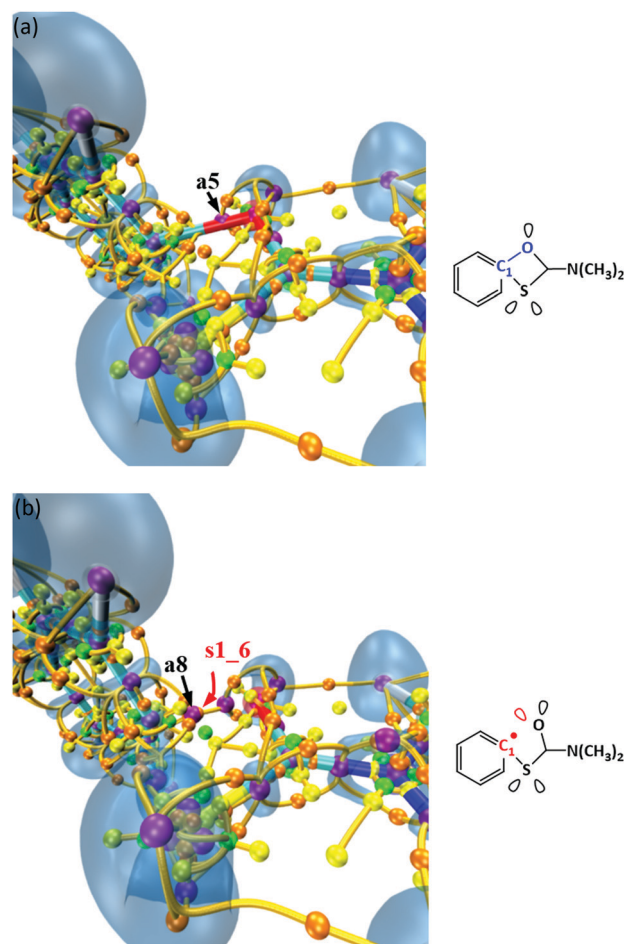

Fig. 4 Extended ELF-molecular graphs together with the Lewis-like structures, including all types of ELF CPs: attractors or maxima in purple, saddles of index one in orange, saddles of index two in yellow and minima or repellors in green; (a) before and (b) after the fifth change. The ELF isosurface (0.85) is also shown.

decreases by two. Therefore, we disagree with Zahedi *et al.*[21] on the description of the C1–S bond formation through a cusp function.

The continuous stretching of the C1–O bond leads to the appearance of the pair (a_8, s_{1_6}) in the vicinity of the ipso–carbon, following the same pattern of the first and second folds. From a topological perspective, this change in the number of ELF CPs marks the onset of the C1–O breaking process, as presented in Fig. 4.

Two saddle points of index one, s_{1_7} and s_{1_8}, and a saddle of index two, s_2, seem to be involved in the subsequent change in the number of ELF CPs, as shown in Fig. 5. However, both the dynamical systems and topology branches provide strong and well-established arguments prohibiting this change from being described in terms of any unfolding.[28,29] It should be stressed that this issue requires special care since it is implicit in the conditions imposed by Thom[23] to deduce the seven unfoldings.[28,29] Monitoring the Hessian at these three points and the relative distance between them along the IRC path reveals that s_{1_7} and s_2 collide and annihilate, whereas s_{1_8}

remains in the molecular graph of the ELF; see the ESI† for detailed information.

By "naked-eye" inspection, it is impossible to determine whether the three CPs, a_8, s_{1_8} and s_{1_9}, are involved in the last crucial change from the ELF-molecular graph, as shown in Fig. 6. Following the value of the Hessian evaluated at these points and their relative distances constitutes the correct methodology to approach this task.[20] In fact, this complementary-like procedure shows that a_8 and s_{1_9} move in opposite directions before the change since their relative separation increases by a factor of 1.02, while a_8–s_{1_8} decreases by about 2 times. Therefore, a_8 and s_{1_8} merge and disappear *via* the sixth fold. This fact means it is the fold-type unfolding (and not the elliptic umbilic, as mis-identified by Zahedi *et al.*[21]) that characterizes all topographical changes associated with electron-pair rearrangements leading to the breaking of the C1–O single bond, since neither a_8 nor s_{1_8} change their index[22] and s_{1_9} plays no role during the chemical event, as shown in the ESI.† Topologically speaking, this last change in the number of ELF CPs completes the migration of the aromatic ring from the oxygen to the sulphur atom.
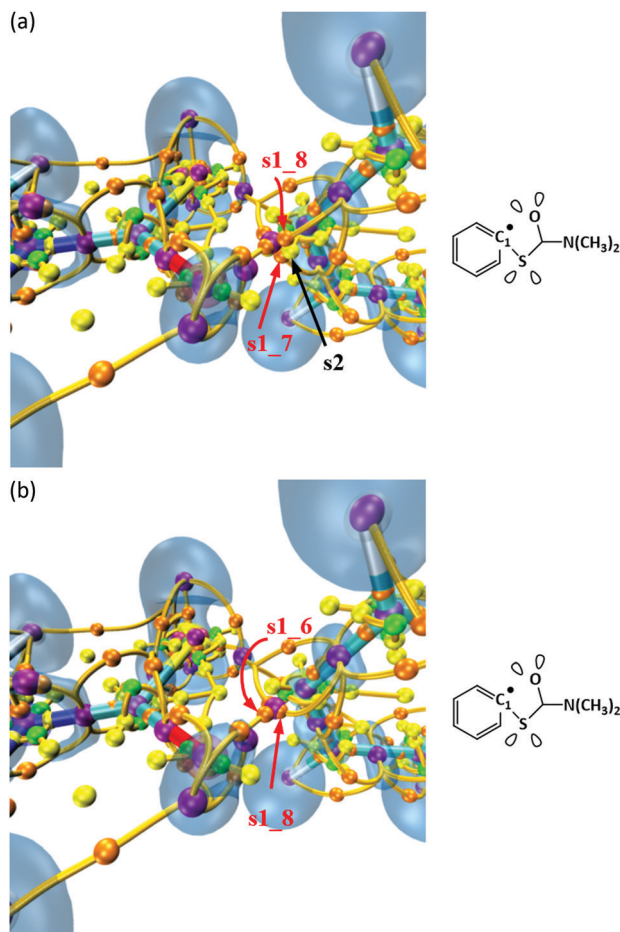
Fig. 5 Extended ELF-molecular graphs together with the Lewis-like structures, including all types of ELF CPs: attractors or maxima in purple, saddles of index one in orange, saddles of index two in yellow and minima or repellors in green; (a) before and (b) after the sixth change. The ELF isosurface (0.85) is also shown.
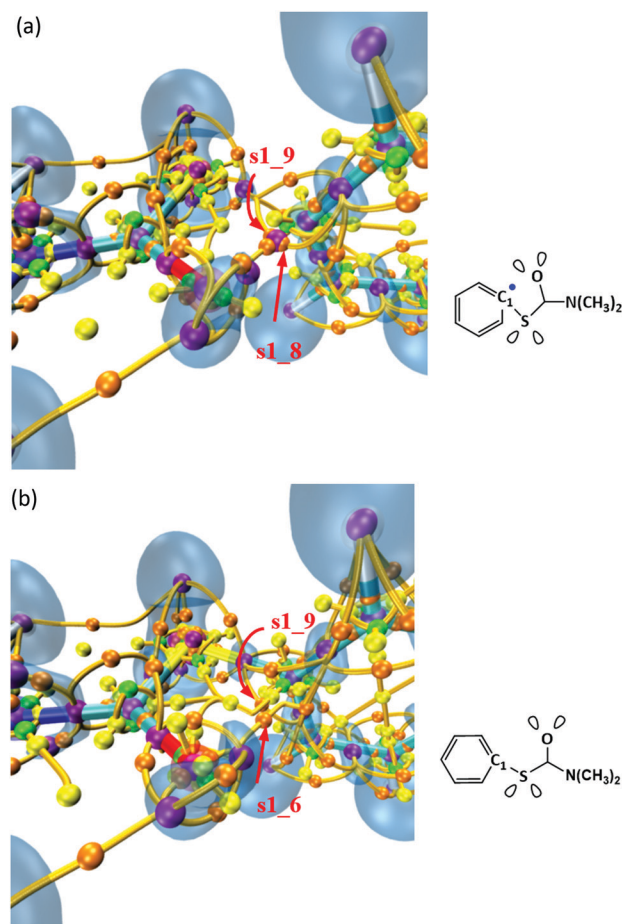

Fig. 6 Extended ELF-molecular graphs together with the Lewis-like structures, including all types of ELF CPs: attractors or maxima in purple, saddles of index one in orange, saddles of index two in yellow and minima or repellors in green; (a) before and (b) after the seventh change. The ELF isosurface (0.85) is also shown.

Scheme 2 summarizes key electron-pair reorganizations for the NKR *via* the Lewis-like structures. Due to the difference in the electronegative character between atoms of each pair: (carbon, sulphur) and (carbon, oxygen), the (C=S) and (C=O) double bonds are only formal (Scheme 1); thus, no topographical change is observed concerning their reduction/ formation. Following the Hessian at potentially involved CPs and their relative distances along the IRC pathway reveals that the fold polynomial describes all significant chemical events (*i.e.*, the breaking/forming processes of the chemical bond), in contrast to previous assignations suggested by Zahedi *et al.*[21] Our recent work[20,24–26] shows that unfoldings are capable of capturing the symmetry features of the electron-pair density, providing an accurate picture of changes in this property along a reactive coordinate. Therefore, one could *a priori* (without any kind of calculation) characterize the breaking and forming of chemical bonds using the correct unfolding. Moreover, evidence in both the ground[20,22] and electronically excited states[24–26] shows that the cusp polynomial characterizes the flow of the electron pairing density in highly symmetrical
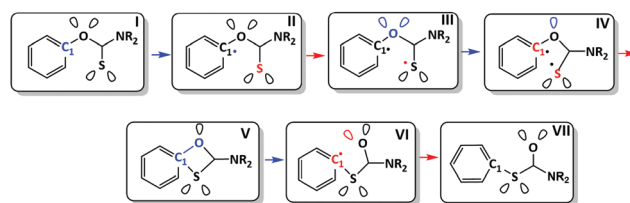
Scheme 2 Lewis-like representation for the key chemical events associated with the Newman–Kwart rearrangement ($R = CH_3$) as derived from the bonding evolution theory framework.

reaction systems, whereas the fold describes remarkable chemical events in low symmetry systems. Nonetheless, characterizing the homolytic bond breaking and forming *via* a cusp demands an *extra* condition; namely, the electron-pair symmetry must be invariant with respect to a plane perpendicular to the stretching/contracting bond throughout the chemical process.[24] This means that homolytic events fail to be a sufficient condition for detecting any flag of a cusp-type

polynomial. Thus, it is reasonable to observe only folds in the NKR since all significant chemical events are heterolytic due to the noticeable electronegativity difference between the involved atoms, which generates a strong polar character in all forming/breaking covalent bonds.

For a more concise analysis, let us now use the arrow-pushing model[30–32] to compare our findings with those of Zahedi *et al.* regarding the formation of the C1–S bond and the C1–O cleavage. The arrow model is a purely intuitive way (*i.e.*, this approach has no experimental support) for representing relevant chemical events. However, this way of rationalizing electron reorganizations leading to significant chemical events is deeply anchored in the minds of chemists, and many chemistry textbooks make use of it. Zahedi *et al.*[21] described the formation of a single bond between the sulphur and the ipso–carbon atoms through an elliptic umbilic function, which means that one attractor becomes a saddle point of index two, and consequently, the electron-pair density flows from its associated basin and accumulates within the basin of another maximum. On the other hand, we rationalized this event *via* a fold polynomial, meaning that no new critical point arises. Both descriptions are identical within the (curly) arrow representation since the electron-pair density is transferred from one disappearing basin to a strengthening one. Nonetheless, the C1–O rupture is quite different in the arrow model. In the vision of Zahedi *et al.*, three CPs merge and a new critical point appears; therefore, one could represent this electron rearrangement using two curly arrows indicating the flow of electron pairing density from both basins into the new one. In contrast, only one curved arrow would suffice for our topological description.

Theory and computational details

BET[22] is a standard tool[20] that combines the topological analysis of the ELF[27] with catastrophe theory[23] to describe the breaking and forming processes of chemical bonds along a reaction path. ELF is usually understood as a local measure of electron kinetic energy excess due to Pauli's exclusion principle,[33–35] and thus provides a partition of the molecular space into regions (called basins) having a direct connection to Lewis theory, such as valence bonds, core and lone pairs.[36–38] Furthermore, these regions surround the ELF's critical points.[38] Such a function displays only four types of CPs since it is defined in $\mathbb{R}^3$:maximum or attractor, saddle of index one, saddle of index two, and minimum or repellor. The appearance and annihilation of ELF CPs along a reaction coordinate are associated with electron reorganization leading to the forming/breaking of chemical bonds through parametric polynomials (unfoldings).[23] The essential feature of CPs that merge and disappear is that the Hessian matrix (evaluated at such points) shows a strong tendency to reach the zero value due to a decrease in the relative distance between points. Moreover, if the Hessian is non-invertible, the evaluated point is typically referred to as a degenerate CP.[23,39] It is crucial to emphasize

that changes in the collection of CPs along a reaction pathway can only be described in terms of unfoldings if some conditions are fulfilled[28,29,40,41] (see the ESI† for further details on the first part of this section).

All calculations were conducted using the Gaussian 16 package of programs[42] following the setup provided by Zahedi *et al.*,[21] *i.e.*, the aug-cc-pvtz basis set was employed with diphenyl ether and chlorobenzene solvent media, each combined with the M06-2X and MN15-L functionals. The absolute temperature values were set at 505 and 413 K for the first and second solvents, respectively. The IRC paths were constructed using a step size value ten times smaller (0.001 amu$^{1/2}$ Bohr) than the default one (0.01 amu$^{1/2}$ Bohr) to clarify the results. The topological analysis of the ELF for each point on the reaction path was performed *via* the Multiwfn program.[43] The images of the topographic map were generated through the VMD software.[44]

Conclusions

The assignment criteria of the unfoldings[23] describing the forming/breaking processes of chemical bonds featuring the Newman–Kwart rearrangement have been re-examined. Monitoring the relative distance between potentially degenerate critical points of the electron localization function and the Hessian matrix evaluated at each point[20,24–26] along the intrinsic reaction coordinate shows that the fold-type unfolding indeed characterizes all relevant chemical events, in contrast to the assertion of Zahedi *et al.*[21] However, our topological description and the one provided by Zahedi *et al.* concerning the formation of a single bond between the ipso–carbon and the sulphur atom are similar within the intuitive arrow model;[30–32] whereas, the rupture of the C1–O bond is quite different. Moreover, the topological procedure evidently shows that the formation of the single bond between the C1 ipso–carbon and sulphur atom occurs before the C1–O heterolytic cleavage; thus, we disagree with Zahedi *et al.* on the order of occurrence of such crucial events. However, careful attention must be paid to changes in the number of critical points driven by coalescing saddle points because such events are prohibited from being described through any unfolding.[28,29,40] Thom[23] succeeded in deducing these polynomials by excluding the possibility of saddle connections.[28,29] The fact that all electron-pair reorganization can be interpreted in terms of the fold function is intimately related to a low electron-pair density symmetry (because the electrical charge is displaced towards the more electronegative atom); consequently, all forming/breaking processes of chemical bonds are heterolytic. As should be expected, such an unfolding happens to be the most common one, encompassing a wide range of reaction systems since no particular condition is required, which means that one can *a priori* choose the suitable polynomial for describing key chemical events. This result is independent of the electronic state of the system, the kinetic order of the reaction, or the regioselectivity, but depends solely on the way

the electron-pair density spans the molecular space and redistributes as the breaking/forming of chemical bonds occur. These findings predict that the unfoldings constitute an unambiguous measure of covalent bond polarity.

Author contributions

L. A.-H., E. C.: project supervision, conceptualization, data analysis, manuscript writing; L. A.-H., C. G., M. D.-N.: calculations, reaction path, characterization; C. G., M. D.-D.: data analysis, calculations. All authors reviewed and commented on the manuscript.

Conflicts of interest

There are no conflicts to declare.

Acknowledgements

References

1 H. Kwart and E. R. Evans, The Thio-Claisen Rearrangement. The Mechanism of Thermal Rearrangement of Allyl Aryl Sulfides, *J. Org. Chem.*, 1966, **31**, 413–419.

2 M. S. Newman and H. A. Karnes, The Conversion of Phenols to Thiophenols via Dialkylthiocarbamates, *J. Org. Chem.*, 1966, **31**, 3980–3984.

3 H. Jacobsen and J. P. Donahue, Expanding the scope of the Newman-Kwart rearrangement - A computational assessment, *Can. J. Chem.*, 2006, **84**, 1567–1574.

4 J. D. Moseley, R. F. Sankey, O. N. Tang and J. P. Gilday, The Newman-Kwart rearrangement re-evaluated by microwave synthesis, *Tetrahedron*, 2006, **62**, 4685–4689.

5 G. C. Lloyd-Jones, J. D. Moseley and J. S. Renny, Mechanism and application of the Newman-Kwart O → S rearrangement of *O*-aryl thiocarbamates, *Synthesis*, 2008, 661–689.

6 J. N. Harvey, J. Jover, G. C. Lloyd-Jones, J. D. Moseley, P. Murray and J. S. Renny, The Newman-Kwart rearrangement of *O*-aryl thiocarbamates: Substantial reduction in reaction temperatures through palladium catalysis, *Angew. Chem., Int. Ed.*, 2009, **48**, 7612–7615.

7 M. Burns, G. C. Lloyd-Jones, J. D. Moseley and J. S. Renny, The molecularity of the Newman-Kwart rearrangement, *J. Org. Chem.*, 2010, **75**, 6347–6353.

8 T. Broese, A. F. Roesel, A. Prudlik and R. Francke, An Electrocatalytic Newman-Kwart-type Rearrangement, *Org. Lett.*, 2018, **20**, 7483–7487.

9 S. Chiniforoush and C. J. Cramer, Quantum Chemical Characterization of Factors Affecting the Neutral and Radical-Cation Newman-Kwart Reactions, *J. Org. Chem.*, 2019, **84**, 2148–2157.

10 C. N. Neumann, J. M. Hooker and T. Ritter, Concerted nucleophilic aromatic substitution with 19F- and 18F-, *Nature*, 2016, **534**, 369–373.

11 S. Brooker, G. B. Caygill, P. D. Croucher, T. C. Davidson, D. L. J. Clive, S. R. Magnuson, S. P. Cramer and C. Y. Ralston, Conversion of some substituted phenols to the corresponding masked thiophenols, synthesis of a dinickel(*n*) dithiolate macrocyclic complex and isolation of some metal- And ligand-based oxidation products, *J. Chem. Soc., Dalton Trans.*, 2000, **2**, 3113–3121.

12 Z. O. D. L. Cristiano and L. Cotarca, Thione–Thiol Rearrangement: Miyazaki–Newman–Kwart Rearrangement and Others, *Pept. Mater.*, 2007, **310**, 1–26.

13 M. Hori, M. Ban, E. Imai, N. Iwata, Y. Suzuki, Y. Baba, T. Morita, H. Fujimura, M. Nozaki and M. Niwa, Novel Nonnarcotic Analgesics with an Improved Therapeutic Ratio. Structure-Activity Relationships of 8-(Methylthio)- and 8-(Acylthio)-1,2,3,4,5,6-hexahydro-2,6-methano-3-benzazocines, *J. Med. Chem.*, 1985, **28**, 1656–1661.

14 A. Gallardo-Godoy, A. Fierro, T. H. McLean, M. Castillo, B. K. Cassels, M. Reyes-Parada and D. E. Nichols, Sulfur-substituted α-alkyl phenethylamines as selective and reversible MAO-A inhibitors: Biological activities, CoMFA analysis, and active site modeling, *J. Med. Chem.*, 2005, **48**, 2407–2419.

15 Z. F. Tao, X. Qian, Y. Zhang and M. Fan, Synthesis of 3*H*-1,8,9-trimethylthieno[3′,2′:6,7]naphtho [2,1-*b*]pyran-3-one with potential photobiological activity, *Dyes Pigm.*, 1998, **37**, 113–119.

16 I. Llarena, A. C. Benniston, G. Izzet, D. B. Rewinska, R. W. Harrington and W. Clegg, Synthesis of a redox-active molecular switch based on dibenzo[1,2]dithiine, *Tetrahedron Lett.*, 2006, **47**, 9135–9138.

17 V. V. Kane, A. Gerdes, W. Grahn, L. Ernst, I. Dix, P. G. Jones and H. Hopf, A novel entry into a new class of cyclophane derivatives: Synthesis of (±)-[2.2]paracyclophane-4-thiol, *Tetrahedron Lett.*, 2001, **42**, 373–376.

18 P. García-García, F. Lay, P. García-García, C. Rabalakos and B. List, A Powerful Chiral Counteranion Motif for Asymmetric Catalysis, *Angew. Chem.*, 2009, **121**, 4427–4430.

19 P. Hohenberg and W. Kohn, Inhomogeneous Electron Gas, *Phys. Rev.*, 1964, **136**, 864–871.

20 L. Ayarde-Henríquez, C. Guerra, M. Duque-Noreña, E. Rincón, P. Pérez and E. Chamorro, Are There Only Fold Catastrophes in the Diels–Alder Reaction Between Ethylene and 1,3-Butadiene?, *J. Phys. Chem. A*, 2021, **125**, 5152–5165.

21 A. S. Zahedi Ehsan, M. Sanie and S. Hosein Ghorbani, Insights into the kinetics and molecular mechanism of the Newman–Kwart rearrangement, *New J. Chem.*, 2021, **45**, 16978–16988.

22 X. Krokidis, S. Noury and B. Silvi, Characterization of Elementary Chemical Processes by Catastrophe Theory, *J. Phys. Chem. A*, 1997, **101**, 7277–7282.

23 R. Thom, *Structural Stability and Morphogenesis*, CRC Press, 1st edn, 1972.

24 C. Guerra, L. Ayarde-Henríquez, M. Duque-Noreña and E. Chamorro, On Electron Pair Rearrangements in Photochemical Reactions: 1,3-Cyclohexadiene Ring Opening, *J. Phys. Chem. A*, 2022, **126**, 395–405.

25 E. C. Cristian Guerra, L. Ayarde-Henríquez and M. Duque-Noreña, Unraveling the Bonding Nature Along the Photochemically Activated Paterno-Büchi Reaction Mechanism, *Chem. Phys. Chem.*, 2021, **22**, 2342–2351.

26 C. Guerra, L. Ayarde-Henríquez, M. Duque-Noreña, C. Cárdenas, P. Pérez and E. Chamorro, On the nature of bonding in the photochemical addition of two ethylenes: C–C bond formation in the excited state?, *Phys. Chem. Chem. Phys.*, 2021, **23**, 20598–20606.

27 A. D. Becke and K. E. Edgecombe, A simple measure of electron localization in atomic and molecular systems, *J. Chem. Phys.*, 1990, **92**, 5397–5403.

28 V. Arnold'd; V. Afrajmovich and I. Yu, L. Shil'nikovn, *Dynamical Systems V*, Springer-Verlag, Berlin Heidelberg, 1st edn, 1994, vol. **5**.

29 R. Gilmore, *Catastrophe theory for scientists*, Dover Publications, 1st edn, 1993.

30 V. Polo, J. Andrés, R. Castillo, S. Berski and B. Silvi, Understanding the molecular mechanism of the 1,3-dipolar cycloaddition between fulminic acid and acetylene in terms of the electron localization function and catastrophe theory, *Chem. – Eur. J.*, 2004, **10**, 5165–5172.

31 J. Andrés, P. González-Navarrete and V. S. Safont, Unraveling reaction mechanisms by means of Quantum Chemical Topology Analysis, *Int. J. Quantum Chem.*, 2014, **114**, 1239–1252.

32 J. Andrés, S. Berski and B. Silvi, Curly arrows meet electron density transfers in chemical reaction mechanisms: from electron localization function (ELF) analysis to valence-shell electron-pair repulsion (VSEPR) inspired interpretation, *Chem. Commun.*, 2016, **52**, 8183–8195.

33 Y. Grin, A. Savin and S. Bernard, The ELF Perspective of Chemical Bonding, in *The Chemical Bond: Fundamental Aspects of Chemical Bonding*, ed. G. Frenking and S. Shaik, Wiley-VCH Verlag GmbH & Co. KGaA, 1st edn, 2014, pp. 345–382.

34 P. Fuentealba, E. Chamorro and J. C. Santos, Understanding and using the electron localization function, in *Theoretical and Computational Chemistry*, A. Toro-Labbé, Elsevier B.V., 1st edn, 2007, pp. 57–85.

35 J. Andrés, P. González-Navarrete, V. S. Safont and B. Silvi, Curly arrows, electron flow, and reaction mechanisms from the perspective of the bonding evolution theory, *Phys. Chem. Chem. Phys.*, 2017, **19**, 29031–29046.

36 F. Fuster, A. Savin and B. Silvi, Topological Analysis of the Electron Localization Function (ELF) Applied to the Electrophilic Aromatic Substitution, *Can. J. Chem.*, 1996, **74**, 1088–1096.

37 B. Silvi, The synaptic order: A key concept to understand multicenter bonding, *J. Mol. Struct.*, 2002, **614**, 3–10.

38 R. J. Gillespie, S. Noury, J. Pilmé and B. Silvi, An Electron Localization Function Study of the Geometry of d0 Molecules of the Period 4 Metals Ca to Mn, *Inorg. Chem.*, 2004, **43**, 3248–3256.

39 I. Poston and T. Stewart, *Catastrophe Theory and its Applications*, Pitman Publishing Limited, California, 1st edn, 1979.

40 M. M. Peixoto, Structural stability on two-dimensional manifolds, *Topology*, 1962, **1**, 101–120.

41 S. Albeverio, J. B. Alblas, S. A. Amitsur, I. J. Bakelman, G. Bakker, J. W. de Bakker, C. Bardos, H. Bart, H. Bass, A. Bensoussan, M. Bercovier, L. Berkovitz, M. Berger, E. A. Bergshoeff, E. Bertin, F. Beukers, A. Beutelspacher, H. P. Boas, J. Bochnak, H. J. M. Bos, B. L. J. Braaksma, T. P. Branson, D. S. Bridges, A. E. Brouwer, M. G. de Bruin, R. G. Bums, H. Capel, P. Cartier, C. Cercignani, J. M. C. Clark, Ph. Clement, A. M. Cohen, J. W. Cohen, P. Conrad, H. S. M. Coxeter, R. F. Curtain, M. H. A. Davis, M. V. Dekster, C. Dellacherie, G. van Dijk, H. C. Doets, I. Dolgachev, A. Dress, J. J. Duistermaat, D. van Dulst, H. van Duyn, H. Dym, A. Dynin, M. L. Eaton, W. Eckhaus, P. van Emde Boas, H. Engl, G. Ewald, V. I. Fabrikant, A. Fasano, M. Fliess, R. M. Fossum, B. Fuchssteiner, G. B. M. van der Geer, R. D. Gill, V. V. Goldberg, J. de Graaf, J. Grasman, P. A. Griffith, A. W. Grootendorst, L. Gross, P. Gruber, K. P. Hart, G. Heckman, A. J. Hermans, W. H. Hesselink, C. C. Heyde, M. W. Hirsch, K. H. Hofmann, A. T. de Hoop, P. J. van der Houwen, N. M. Hugenholtz, J. R. Isbell, A. Isidori, E. M. de Jager, D. Johnson, P. T. Johnstone, D. Jungnickel, M. A. Kaashoek, V. Kac, W. L. J. van der Kallen, D. Kanevsky, Y. Kannai, H. Kaul, E. A. de Kerf, W. Klingenberg, T. Kloek, J. A. C. Kolk, G. Komen, T. H. Koomwinder, L. Krop, B. Kuperschmidt, H. A. Lauwerier, J. van Leeuwen, H. W. Lenstra Jr., J. K. Lenstra, H. Lenz, M. Levi, J. Lindenstrauss, J. H. van Lint, F. Linton, A. Liulevicius, M. Livshits, W. A. J. Luxemburg, R. M. M. Mattheij, L. G. T. Meertens, I. Moerdijk, J. P. Murre, H. Neunzert, G. Y. Nieuwland, G. J. Olsder, B. ørsted, F. van Oystaeyen, B. Pareigis, K. R. Parthasarathy, K. R. Parthasarathy, I. I. Piatetskii-Shapiro, H. G. J. Pijls, N. U. Prabhu, E. Primrose, A. Ramm, C. M. Ringel, J. B. T. M. Roerdink, K. W. Roggenkamp, G. Rozenberg, W. Rudin, S. N. M. Ruysenaars, A. Salam, A. Salomaa, P. Saunders, J. P. M. Schalkwijk, C. L. Scheffer, R. Schneider, J. A. Schouten, F. Schurer, J. J. Seidel, A. Shenitzer, V. Snaith, T. A. Springer, J. H. M. Steenbrink, J. D. Stegeman, F. W. Steutel, P. Stevenhagen, I. Stewart, R. Stong, L. Streit, K. Stromberg, L. G. Suttorp, D. Tabak, F. Takens, R. J. Takens, N. M. Temme, S. H. Tijs, B. Trakhtenbrot, N. S. Tmdinger, L. N. Vaserstein, M. L. J. van de Vel, F. D. Veldkamp, W. Vervaat, P. M. B. Vitanyi, N. J. Vlaar, H. A. van der Vorst, J. de Vries, F. Waldhausen, B. Wegner, J. J. O. O. Wiegerinck, J. C. Willems, J. M. Wills, B. de Wit, S. A. Wouthuysen, S. Yuzvinskii and L. Zalcman, *Encyclopaedia of Mathematics*, Kluwer Academic Publishers, Dordrecht, 1991.

42 M. A. M. J. Frisch, G. W. Trucks, H. B. Schlegel, G. E. Scuseria, G. A. Robb, J. R. Cheeseman, G. Scalmani, V. Barone, B. Mennucci, J. B. Petersson, H. Nakatsuji, X. Li,

M. Caricato, A. V. Marenich, J. V. O. B. G. Janesko, R. Gomperts, B. Mennucci, H. P. Hratchian, F. A. F. Izmaylov, J. L. Sonnenberg, D. Williams-Young, F. Ding, D. Lipparini, F. Egidi, J. Goings, B. Peng, A. petrone, T. Henderson, W. L. Ranasinhe, V. G. Zakrzewski, J. Gao, N. Rega, G. Zheng, T. M. Hada, M. Ehara, K. Toyota, R. Fukuda, J. Hasegawa, M. Ishida, J. A. Nakajima, Y. Honda, O. Kitao, H. Nakai, T. Vreven, K. Throssell, E. Montgomery Jr., J. E. Peralta, F. Ogliaro, M. Bearpark, J. J. Heyd, R. K. N. Brothers, K. N. Kudin, V. N. Staroverov, T. A. Keith, S. S. I. J. Normand, K. Raghavachari, A. Rendell, J. C. Burant, J. J. Tomasi, M. Cossi, J. M. Millam, M. Klene, C. Adamo, R. Cammi, J. B. F. W. Ochterski, R. L. Martin, K. Morokuma, Ö. Farkas and D. J. Fox, R. B. 0. Gaussian 16, 2017.

43 T. Lu and F. Chen, Multiwfn: A multifunctional wavefunction analyzer, *J. Comput. Chem.*, 2012, **33**, 580–592.

44 K. S. W. Humphrey and A. Dalke, VMD: visual molecular dynamics, *J. Mol. Graphics*, 1996, **14**, 33–38.